Atlas-based method for segmentation of cerebral vascular trees from phase-contrast magnetic resonance angiography

Nicolas Passat, Christian Ronse, Joseph Baruthio, Jean-Paul Armspach, Claude Maillot, Christine Jahn

Atlas-based method for segmentation of cerebral vascular tree from phase-contrast magnetic resonance angiography

N. Passat*[,a,b], C. Ronse[a], J. Baruthio[b], J.-P. Armspach[b], C. Maillot[c], C. Jahn[d]
[a]LSIIT, UMR 7005 CNRS-ULP, Strasbourg I University, France;
[b]IPB, UMR 7004 CNRS-ULP, Strasbourg I University, France;
[c]Institut d'Anatomie Normale, Strasbourg I University, France;
[d]Service de Radiologie, Hôpitaux Universitaires de Strasbourg, France

ABSTRACT

Phase-contrast magnetic resonance angiography (PC-MRA) can produce phase images which are 3-dimensional pictures of vascular structures. However, it also provides magnitude images, containing anatomical - but no vascular - data. Classically, algorithms dedicated to PC-MRA segmentation detect the cerebral vascular tree by only working on phase images. We propose here a new approach for segmentation of cerebral blood vessels in PC-MRA using the two types of images. This approach is based on the hypothesis that a magnitude image contains anatomical information useful for vascular structures detection. That information can then be transposed from a normal case to any patient image by image registration. An atlas of the whole head has been developed in order to store such anatomical knowledge. It divides a magnitude image into several "vascular areas", each one having specific vessel properties. The atlas can be applied on any magnitude image of an entire or nearly entire head by deformable matching, thus helping to segment blood vessels from the associated phase image. The segmentation method used afterward is composed of a topology-conserving region growing algorithm using adaptative threshold values depending on the current region of the atlas. This algorithm builds the arterial and venous trees by iteratively adding voxels which are selected according to their greyscale value and the variation of values in their neighborhood. The topology conservation is guaranteed by only selecting simple points during the growing process. The method has been performed on 15 PC-MRA of the brain. The results have been validated using MIP and 3D surface rendering visualization; a comparison to other results obtained without atlas proves that atlas-based methods are an effective way to optimize vascular segmentation strategies.

Keywords: atlas-based segmentation, adaptative region growing, simple points, magnetic resonance angiography, cerebral vascular tree

1. INTRODUCTION

Magnetic Resonance Angiography (MRA) is a non-invasive technique[1] providing high-quality 3D images of vascular structures. The two kinds of techniques designed to visualize venous and arterial blood vessels are Time-Of-Flight MRA[2] (TOF-MRA) and Phase-Contrast MRA[3] (PC-MRA). Those techniques are frequently used to study the vascular structures of the brain. Indeed, the availability of precise information about the brain vascular network is fundamental for planning and performing neurosurgical procedures, but also for detecting pathologies such as aneurysms and stenoses. Despite of the development of numerous methods to perform blood vessel segmentation from MRA, there is still none being able to provide completely satisfactory results for a whole cerebral vascular tree, which contains large and small vessels presenting very different and sometimes inhomogeneous intensity values. Since all classical image processing tools have been applied more or less successfully to the case of vessels segmentation, it might be interesting to explore a new kind of algorithms, involving a priori knowledge about image acquisition or anatomic structures. In this paper, we propose a first attempt to use anatomic knowledge as a way to guide a segmentation algorithm. The result of this attempt is a new method for segmentation of vascular structures of the brain and the entire head from 3D PC-MRA. It is composed of an adaptative region growing algorithm using an atlas of vascular areas of the head. This paper is organized as follows. In Section 2, we review previous approaches concerning vessels segmentation in 3D angiographic images. In Section 3, the way to integrate a priori knowledge in such algorithms is discussed and an atlas is

*passat@dpt-info.u-strasbg.fr; phone (+33)3 90 24 45 56

described as a solution to modelize anatomic knowledge. In Section 4, we describe the proposed algorithm, based on this vascular atlas and an adaptative region growing method. In section 5, technical details concerning the segmentation process and the database used for its validation are provided. In Section 6, the method is tested on this 15 PC-MRA database. The results are analyzed and compared to results obtained with two other region growing algorithms. Discussion and projects are presented in Section 7.

2. RELATED WORK

Several methods related to vascular network segmentation from 3D angiographic data have been published for the last 15 years. They can be divided into eight categories, corresponding to the main strategies used to carry out the segmentation[†]: filtering, mathematic morphology, region growing, vessel tracking, differential analysis, deformable models, statistical analysis and artificial intelligence. The following description only gives a tiny part of the existing methods for each category.

Some of the proposed algorithms use filtering to segment blood vessels, or only to improve their visualization in 3D medical images. Orkisz et al.[4] propose a 3D spatial filtering technique searching the local orientation of the vessel and then performing nonlinear smoothing in this direction. Du et al.[5] approximate vessels as cylinder segments of finite width in order to propose filters of specific size dedicated to noise removing. A second kind of methods uses mathematic morphology. A grey-level morphological filter, based on erosion and dilatation operators is proposed by Cline et al.[6] to segment coronary angiography images. Yim et al.[7] propose small vessel path detection by performing a grey-scale skeletonization considering 3D images as acyclic graphs. Watershed segmentation is also used by Kobashi et al.[8] as a first segmentation step before classifying primitives. Region growing is another way to perform blood vessel segmentation. Zahlten et al.[9] use such a strategy to segment the liver vascular tree and to generate a graph of its structure. Dokládal et al.[10] add a constraint to preserve the topology of this structure, only allowing simple points to be added during the growing process. Vessel tracking methods have also been studied, especially by Flasque et al.[11] who use an adaptative box to iteratively detect the vessels and their bifurcations. Sato et al.[12] and Krissian et al.[13] propose multiscale tools for segmenting vessel centrelines by analyzing the differential properties of the images (eigenvalues and eigenvectors). Lorigo et al.[14] perform a segmentation of cerebral MRA by a deformable model based approach using level sets. Deformable models using B-spline are also proposed by Frangi et al.[15] to detect central vessel axis and vessel walls. Some statistical approaches, developed by Chung et al.[16] and Wilson et al.[17] use gaussian or rician intensity distributions to segment the vessels by applying an Expectation-Maximization algorithm. The last category of methods integrates artificial intelligence concepts to perform vessel segmentation, as the one proposed by Kobashi et al.,[8] where artificial neural networks are used while a minimum cost path approach is performed to segment vessels even in case of stenosis.

The algorithm proposed in this article is inspired from the growing method described in Dokládal's[10] paper. However, it is quite different while we propose to add an intensity variation criterion which makes the segmentation more robust, and to use an atlas to allow adaptative threshold values.

3. A PRIORI KNOWLEDGE INTEGRATION

3.1. Currently used knowledge

As described in the previous section, there exist various methods dedicated to vascular structures segmentation, using different strategies. Nevertheless all of them use very little a priori knowledge. Indeed they are generally based on three simple concepts:

- vessels (*i.e.* flowing blood) correspond to the voxels of highest intensity value in MRA images;
- vessels are supposed to have a tubular shape (even if this assumption is approximative and sometime false);

[†]Many other criterions could be chosen to classify the existing algorithms: automaticity, kind of data being processed, centreline or whole vessel detection, size of the searched vessels, general methods or methods dedicated to a particular organ, etc...

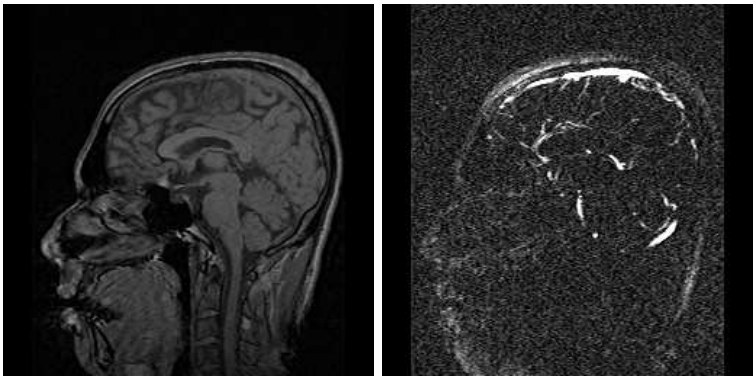

Figure 1. Slices of the two images provided by one PC-MRA acquisition. The left picture is the magnitude image containing anatomical, but no vascular information. The right picture is the phase image, only containing vascular information plus noise and artefacts. Usually, only that second image is used during the segmentation process.

- vascular networks are organized in a tree structure.

Using high level a priori knowledge could be an efficient way to make segmentation tools more reliable than they currently are. Two kinds of a priori knowledge can allow such improvement: knowledge concerning image acquisition techniques and knowledge concerning the studied anatomic structures. We propose here to use that second kind of knowledge in order to modelize and integrate parts of it in a segmentation method. Modelization and integration are performed by using a vascular atlas of the head.

3.2. Vascular atlas

The main purpose of this work is to take the advantage of the bimodality of the same PC-MRA, using the magnitude image to integrate anatomical knowledge. The integration of anatomical knowledge into the segmentation of vascular structures has two main implications: to find an accurate way of modelization and to determine the rules for its correct use. The solution proposed here consists in using an atlas especially designed in order to segment PC-MRA images. PC-MRA provides two different images for a same acquisition: a phase image only containing information on flowing blood, and a magnitude image which does not contain any vascular information but anatomical one, as a classical MRI image. An example of those two kinds of images is given in Figure 1. Therefore PC-MRA provides not only vascular data but also precious information concerning all the head structures of the patient. This bimodality is quite important. Actually, between two patients, the main blood vessels and their branches exhibit much variability, making it nearly impossible to design an atlas only based on vascular structures contained in phase images. As it is quite impossible to find invariant properties by only using vascular images of the head, an idea is to find such invariant properties concerning the relative positions of blood vessels and non-vascular structures of the brain and the head, thus allowing using magnitude images. Indeed, non-vascular structures of the head (and more especially of the brain) are much less variable from one patient to another and easy to localize on anatomical images. This strategy has permitted to develop a vascular atlas no longer based on a phase image, but on a magnitude one. This atlas uses a $256 \times 256 \times 170$ PC-MRA magnitude image of a healthy 25 year old male subject and has been created with semi-automated tools provided by the Medimax software platform[‡]. It first divides the image into four regions, containing arteries, veins, both arterial and venous blood vessels, or no vascular structures. These four regions are then refined into smaller ones (14 different areas), each of them having relatively homogeneous properties according to:

- vessels size (which has a strong influence on their intensity in phase images);
- vessels orientation;

[‡]Medimax is a 3D medical image processing software developed by the IPB. It is available on the internet at `http://www-ipb.u-strasbg.fr/`.

Input: $f_{pha} : [1, dim_x] \times [1, dim_y] \times [1, dim_z] \rightarrow [a, b]$: phase image λ: threshold value ($a \leq \lambda \leq b$) s: seed point ($s \in Def(f_{pha}) = [1, dim_x] \times [1, dim_y] \times [1, dim_z]$)
Output: X: vascular binary image (X is considered as a set)

$X := \{s\}$
$F := \{L_a, L_{a+1}, ..., L_b\}$ (set of empty FIFO lists)
for (all $y \in N(s)$) ($N(s)$ is the neighborhood of s in $Def(f_{pha})$)
add y in $L_{f_{pha}(y)}$
repeat
$i := Max\{k \in [a, b] \mid L_k \neq \emptyset\}$
remove x from L_i
if (x is simple) then
if ($f_{pha}(x) \geq \lambda$)
$X := X \cup \{x\}$
for (all $y \in N(x) \setminus X$)
if ($y \notin L_{f_{pha}(y)}$)
add y in $L_{f_{pha}(y)}$
until ($f_{pha}(x) < \lambda$)

Table 1. Region growing algorithm proposed in Dokládal's[10] paper.

- vessels position relatively to specific brain or head structures.

This atlas is then used in an adaptative region growing method presented in the following section.

4. METHOD

4.1. Initial algorithm: a region growing process

The method exposed in this paper is inspired from an algorithm[10] proposed by Dokládal et al. It is a region growing algorithm applied to the segmentation of the liver vascular tree from X-ray images. This algorithm starts from a seed point interactively defined as making part of the vascular tree, and iteratively adds simple points[§] chosen in a priority queue according to their intensity. The algorithm, which will be referred to as Alg_1, is summarized in Table 1.

The major advantage of this method is that the use of simple points guarantees that the segmented vascular tree will be topologically correct, with no hole and no cavity. Nevertheless, this strategy also presents two main drawbacks. First, it uses only one seed point. Thus it is possible that a whole part of the vascular tree may be lost during the segmentation process if that part is disconnected from the part containing the seed point, for example by an artefact or a signal loss due to aliasing. Second, the proposed algorithm uses only one constant threshold value. Thus, in order to segment small vessels, presenting a low intensity, one has to accept to also segment noisy areas of the same intensity, connected to the vascular tree. Such behavior can produce many segmentation errors. On the contrary, choosing a high threshold value allowing removing noise will cause the loss of small vessels.

4.2. Optimization: double threshold and intensity variation criterion

We describe here a preliminary optimization to correct the two problems described in the previous subsection. The proposed optimization no longer uses one seed point but multiple seed points chosen by considering a first threshold value λ_{max}. These points are then iteratively used to initialize region growing processes similar to Dokládal's one, with a second threshold λ_{min} lower than λ_{max}. In the previous algorithm, candidate points presenting an intensity higher than the chosen threshold value λ were considered as making part of vascular structures, while the other were rejected. In that proposed optimization, three cases can occur: the candidate point intensity can be lower than λ_{min}, higher than λ_{max} or between the two values. In the first case, the point is rejected while it can be accepted as making part of the vascular structures in the second one, if it preserves

[§]Simple points are points that can be added to an object or removed from it without modifying its current topology. The definition of simple points can be found in many papers[18] dealing with discrete topology.

the vessels topology. In order to deal with the last case, an intensity variation criterion has been introduced to decide whether a candidate point can be chosen or not. This criterion consists in comparing intensities of the candidate point and its already segmented neighbors. The choice process including that criterion can then be summarized as follows.

Let λ_{min} and λ_{max} be the two chosen threshold values. Let α_{min} and α_{max} be the two criterion values chosen (with $0 < \alpha_{min} < \alpha_{max} < 1$). Let x be the candidate voxel and $V(x)$ its neighborhood (the 26 adjacent voxels). For any point a let $I(a)$ be the intensity of a. Let S be the region already segmented. Then if x is a simple point:

- if $(I(x) > \lambda_{max})$ then x is accepted;
- if $(I(x) < \lambda_{min})$ then x is rejected;
- if $(\lambda_{min} \leq I(x) \leq \lambda_{max})$:
  1. if $\exists y \in V(x) \cap S \mid (I(x) < \alpha_{min} I(y))$ then x is rejected;
  2. if not (1.) and $(\exists y \in V(x) \cap S \mid I(x) > \alpha_{max} I(y))$ then x is accepted;
  3. if not (1.) and not (2.) then x is put back in a waiting list until $V(x) \cap S$ is modified.

This criterion forbids to accept a point if its intensity is too low compared to its neighbors which already make part of the segmented structure. This is justified by the fact that a strong reduction of signal generally characterizes the vessel borders in angiographic images. It has been experimentally observed that values $(\frac{1}{2}, \frac{2}{3})$ for $(\lambda_{min}, \lambda_{max})$ give satisfactory results.

The modified algorithm, using two threshold values and an intensity variation criterion is supposed to solve the previous problems. Using several seed points allows segmenting multiple regions which would be lost by using a unique seed point. Nevertheless, a consequence of using several seed points is that the final vascular structure, if more complete, is composed of multiple connected components. Such a structure, that is no longer a tree, is not topologically correct, and could be considered as less satisfactory than the results obtained with the previous method. But even if the presence of multiple components can appear as a weakness, one has to remember that:

- $n - 1$ of the n disconnected components segmented by that method would have been forgotten by the previous one;
- the segmented structure still does not present any hole or cavity, thus preserving two correct topological properties;
- using a double threshold is an effective way to segment structures presenting a low intensity while avoiding to segment noise, which could not be correctly done with the first method.

This optimization, referred to as Alg_2, can be compared to the introduction of a hysteresis thresholding in the growing process, in the way that two threshold values are used instead of one. If that new method can be considered as theoretically better than the previous one, it still does not integrate any a priori knowledge. Moreover, even if it now uses two threshold values, those values are still fixed. To make the algorithm more robust to intensity variations, it might be interesting that these values be adaptative. This is what is done by using the proposed vascular atlas.

4.3. Atlas-based algorithm

Blood vessels intensity varies according to blood velocity, which itself depends on vessels size. The size of vessels of the brain, and more generally of the whole head exhibits much variability. It depends on the vessels position, for example, carotid arteries in the neck, or vessels located in the falx cerebri have very different diameters. One of the informations provided by the developed atlas is the way to estimate the expected intensity of vessels according to their localization in each one of its 14 areas. The following atlas-based algorithm (which will be referred to as Alg_3 from now) can be divided into three steps:

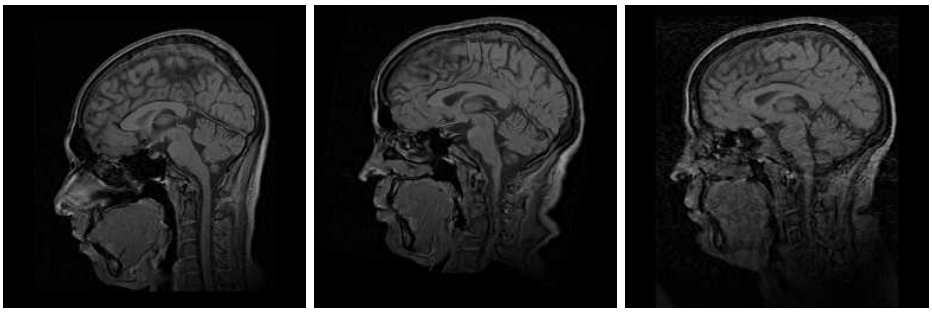

Figure 2. Result provided by the non rigid registration used in the proposed algorithm. Left, magnitude image of the standard case (used to create the atlas). Right, magnitude image of a patient case. Middle, result obtained by non-rigid registration of the left image on the right one. The deformation field used here to obtain that image is then used to map the atlas on the phase image of the patient.

1. First, the magnitude PCA image of a healthy subject is compared to the magnitude image of the current patient, by deformable matching. This first step provides a 3D deformation field that is then used to modify the initial vascular atlas, fitting it to the patient. The new obtained atlas will then give information adapted to the patient's blood vessels. A result provided by the non-rigid registration[19] is illustrated in Figure 2.

2. The deformed atlas is superimposed on the phase image of the patient and the threshold values of each region are then estimated. During this step, the threshold values of each region can be interactively chosen by the user. Nevertheless, they can also be automatically computed using a histogram analysis. This process consists in calculating the histogram for each region of the image. Each histogram is then normalized, and two threshold values are chosen by using heuristic rules directly on the histogram or, more frequently, on its derivative function. All the heuristic rules have been defined by observation and learning on a 10 images database (the 10 images are not the same as the ones used for the final validation).

3. The last step is the vessel segmentation by region growing presented in Table 2. This step is quite similar to Alg_2. The difference is the use of adaptative threshold values during the region growing process. They permit to adapt the segmentation to the current region, allowing, for example, to remove more noise or to detect more efficiently small vessels which could not be found with global threshold values.

All the algorithms presented in this section have been implemented on the Medimax software platform[¶] and all use the ImLib3D[‖] open source C++ library.

5. EXPERIMENTAL SECTION

5.1. Data acquisition

A 15 PC-MRA database has been used to validate the efficiency of the proposed atlas based-algorithm. The MRA examinations were performed on a 1 Tesla whole-body scanner (Gyroscan NT/INTERA 1.0 T from Philips, gradient slope 75 $T/m/s$). The flow encoding sequence called T1FFE/PCA uses a TR of 10 ms and a TE of 6.4 ms. The pool of patients was composed of males and females aged from 21 to 51. The acquired images of dimensions varying between $256^2 \times 150$ and $256^2 \times 180$ voxels, are made of non isotropic voxels. It has to be noticed that in each image, the vascular information only represents 50 000 to 150 000 voxels, *i.e.* approximately 1% of the image.

[¶] All figures presented in this paper have also been computed and visualized with Medimax.

[‖] `http://imlib3d.sourceforge.net/`

```
Input:
    f_pha : [1, dim_x] × [1, dim_y] × [1, dim_z] → [a, b]: phase image
    α_max: intensity variation value (0 < α_max < 1)
    α_min: intensity variation value (0 < α_min < α_max)
Data provided by atlas application:
    λ_max : [1, dim_x] × [1, dim_y] × [1, dim_z] → [a, b]: threshold value
    λ_min : [1, dim_x] × [1, dim_y] × [1, dim_z] → [a, b]: threshold value
Output:
    X: vascular image (binary image) (X is considered as a set)
X := ∅
for (all x ∈ Def(f_pha) = [1, dim_x] × [1, dim_y] × [1, dim_z])
  if (f_pha(x) > λ_max(x))
    if (x ∉ X)
      F := {L_a, L_{a+1}, ..., L_b} (set of empty FIFO lists)
      Refused := ∅
      X := X ∪ {x};
        for (all y ∈ N(x) \ X)
          add y in L_{f_pha(x)}
            repeat
              i := Max{k ∈ [a, b] | L_k ≠ ∅}
              remove x from L_i
              if (x simple) then
                if (x ∉ Refused) then
                  case
                    (f_pha(x) > λ_max(x))
                      X := X ∪ {x}
                      for (all y ∈ N(x) \ X)
                        if (y ∉ L_{f_pha(y)})
                          add y in L_{f_pha(y)}
                    (f_pha(x) < λ_min(x))
                      do nothing
                    (λ_min(x) ≤ f_pha(x) ≤ λ_max(x))
                      if ∃z ∈ N(x) ∩ X.f_pha(x) < α_min(x)f_pha(z)
                        Refused := Refused ∪ {x}
                      else if (∃z ∈ N(x) ∩ X.f_pha(x) > α_max f_pha(z))
                        X := X ∪ {x}
                        for (all y ∈ N(x) \ X)
                          if (y ∉ L_{f_pha(y)})
                            add y in L_{f_pha(y)}
                      else
                        do nothing
              until (f_pha(x) < λ_max(x))
```

Table 2. Third step of the atlas-based region growing algorithm.

5.2. Automaticity

Even if the heuristic values used in step 2 of the atlas-based algorithm do not necessarily provide the best threshold values, they are generally relatively close to them. Steps 1 and 3 being automatic, it is then possible to use the atlas-based algorithm in an entirely automatic fashion. Nevertheless one can choose to manually define the threshold values, or to use the algorithm a second time after an automatic segmentation to correct some of them. A full automation attempt has been carried out on Alg_1 and Alg_2, with no satisfactory results. This failure has been attributed to the difficulty to find invariant criterions allowing to obtain good *global* threshold values. This lack of automaticity is one of the drawbacks when trying to treat each specific part of an image in the same way.

5.3. Segmentation complexity and computation time

Alg_1, Alg_2 and the third step of Alg_3 are quite similar and then have the same complexity of $O(N)$ where N is the number of voxels contained in the image. The second step of Alg_3 also presents a complexity of $O(N)$. Concerning the first step of this algorithm, it is impossible to provide complexity information because the algorithm is based on an energy minimization criterion. Then the complexity depends on the processed image.

The images have been segmented with a computer using a 2.4 GHz Pentium IV processor and a memory of 2 GB. The average computation time is 2 minutes for Alg_1 and 4 minutes for Alg_2. The three steps of Alg_3 required 80, 2 and 4 minutes respectively. The atlas-based algorithm is then more time expensive than the other ones. This is due to the non-rigid registration which is absolutely necessary in order to use the atlas

and then integrate a priori knowledge. Even if this apparently elevated time cost can appear as a drawback, it must be balanced with the supplementary information contained in the segmented image and its higher quality. Moreover, the atlas-based algorithm being automatic, it has to process each image only once, while multiple tries must be carried out with the two other algorithms before finding a correct result**.

6. RESULTS AND DISCUSSION

The results obtained with the atlas-based algorithm have been validated by comparison to those provided by Alg_1 and Alg_2. The validation includes a qualitative study concerning the visual quality of the results and a more quantitative analysis in order to know the amount of supplementary information provided by the proposed method. The three algorithms have been tested on each one of 15 PC-MRA of the previously described database. It has to be noticed that images have been automatically treated only once by the atlas-based algorithm, while it has been necessary to process the images several times with the two other methods before finding the best results. Moreover, Alg_1 was used here with multiple seed points, since using only one seed point yielded topologically correct but very poor results.

6.1. Qualitative validation

Maximum Intensity Projection (MIP) and 3D visualization have been used for the qualitative validation, in order to know if their quality was visually increased by the different algorithms.

The three segmentation processes make MIP visualization more easily readable by removing a large part of background noise. As can be observed in the example of results displayed in Figure 3, Alg_2 and Alg_3 allow to see small vessels structures which were mixed with noise in the initial images. Nevertheless, if the atlas based algorithm provides better MIP visualizations than the two other algorithms, it is a hard task to estimate the improvement. The visible difference becomes more important by observing the segmentation results as a 3D object which can be interactively handled. A 3D visualization of an image segmented by the three algorithms can be found in Figure 4. A visual analysis shows that the segmented images obtained with the atlas-based algorithm generally seem to contain less noise and more details and are therefore easier to analyze.

6.2. Quantitative validation

The 15 segmented images provided by the atlas based algorithm have also been analyzed in a more systematic fashion. They have been quantitatively compared to results obtained using Alg_1 and Alg_2. The results are summarized in Table 3.

One can observe that Alg_2 and Alg_3 both detect more voxels than Alg_1, with less segmentation errors. Moreover, even if they both provide approximately the same quantity of false positives†† (voxels erroneously considered as being vascular), the atlas based algorithm provides, in the same time, a larger quantity of correct positives. It has to be noticed that the set of voxels correctly segmented by Alg_2 is nearly always included in the set correctly segmented by Alg_3. Then, in most cases, there is no loss of information induced by the atlas, while in rare cases, small parts of vessels located at the frontier between two regions have been lost. The parts of the vascular tree only segmented by the atlas-based algorithm contain small vessels presenting a diameter close to the voxels dimension, for example arteries located in the falx cerebri or under the brain. Detecting those small vessels is a real improvement, because they are not distinguishable from the noise in the original images. Those results tend to prove that adding information adapted to the currently processed region during the segmentation process is an efficient way to obtain more detailed and precise vascular structures. Some examples of such segmented vascular structures can be found in Figures 5-6.

**Five to ten attempts are necessary before finding correct parameters in Alg_1 and Alg_2. In addition, concerning Alg_1, many successive seed points have to be manually defined in order to detect some important disconnected components.

††The main segmentation errors of Alg_2 and Alg_3 are always caused by very bright artefacts in images. Most of them could be easily classified and removed by adapted post-processing treatments.

	Comm.	Suppl. segmentation			Segmentation errors			Correct segmentation		
		Alg_1	Alg_2	Alg_3	Alg_1	Alg_2	Alg_3	Alg_1	Alg_2	Alg_3
1	30 951	2 384	27 799	30 960	1 092	0	0	1 292	27 799	30 960
2	44 743	1 448	24 349	35 253	972	0	527	476	24 349	34 726
3	46 669	2 001	14 013	19 988	512	0	0	1 489	14 013	19 988
4	24 045	3 583	18 609	17 006	2 216	0	0	1 367	18 609	17 006
5	27 275	1 828	33 625	34 480	1 031	10	0	797	33 617	34 480
6	13 454	2 873	13 888	44 206	1 956	0	2 006	917	13 888	42 200
7	18 728	3 255	16 985	28 464	2 826	0	140	429	16 985	28 324
8	73 780	6 868	12 012	29 929	2 074	2 074	0	4 794	9 938	29 929
9	83 030	10 156	2 796	30 949	3 078	2 547	2 547	7 078	249	28 402
10	31 166	2 044	7 282	23 517	825	14	1 424	1 219	7 268	22 093
11	26 213	1 472	5 970	17 363	421	0	0	1 051	5 970	17 363
12	34 942	2 506	17 734	29 264	1 588	0	0	918	17 734	29 264
13	31 136	3 244	22 461	29 945	3 093	7 077	4 079	151	15 384	25 866
14	31 931	5 115	4 988	27 228	4 104	0	0	1 011	4 988	27 228
15	23 974	7 305	5 315	26 115	4 925	0	40	2 380	5 315	26 075
Av.	36 136	3 738	15 189	28 318	2 048	782	718	1 692	14 408	27 596

Table 3. Atlas based algorithm (Alg_3) compared with Dokladal's algorithm (Alg_1) and its optimization (Alg_2). The second column (Comm.) indicates how many voxels have been simultaneously segmented by the three algorithms. The next three columns (Suppl. segmentation) indicate how many supplementary voxels have been segmented by each method. The six remaining columns (Segmentation errors, Correct segmentation) indicate, for each method, how many of those supplementary voxels are true or false positives of segmentation. The last line (Av.) provides the average values.

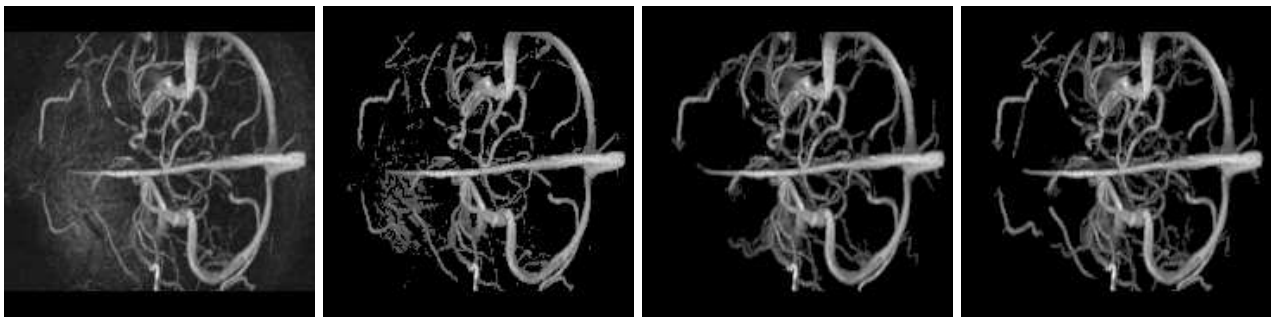

Figure 3. MIP visualization of 3D top view of brain vasculature. From left to right: reconstruction from the original phase image, image segmented by Alg_1, image segmented by Alg_2, image segmented by the atlas based algorithm. The atlas based algorithm visibly gives the best results, removing more noise and conserving more vascular information than Alg_1 and Alg_2.

Figure 4. 3D visualization. From left to right: image segmented by Alg_1, image segmented by Alg_2, image segmented by the atlas based algorithm. The atlas based algorithm provides more vascular information than Alg_1 and Alg_2.

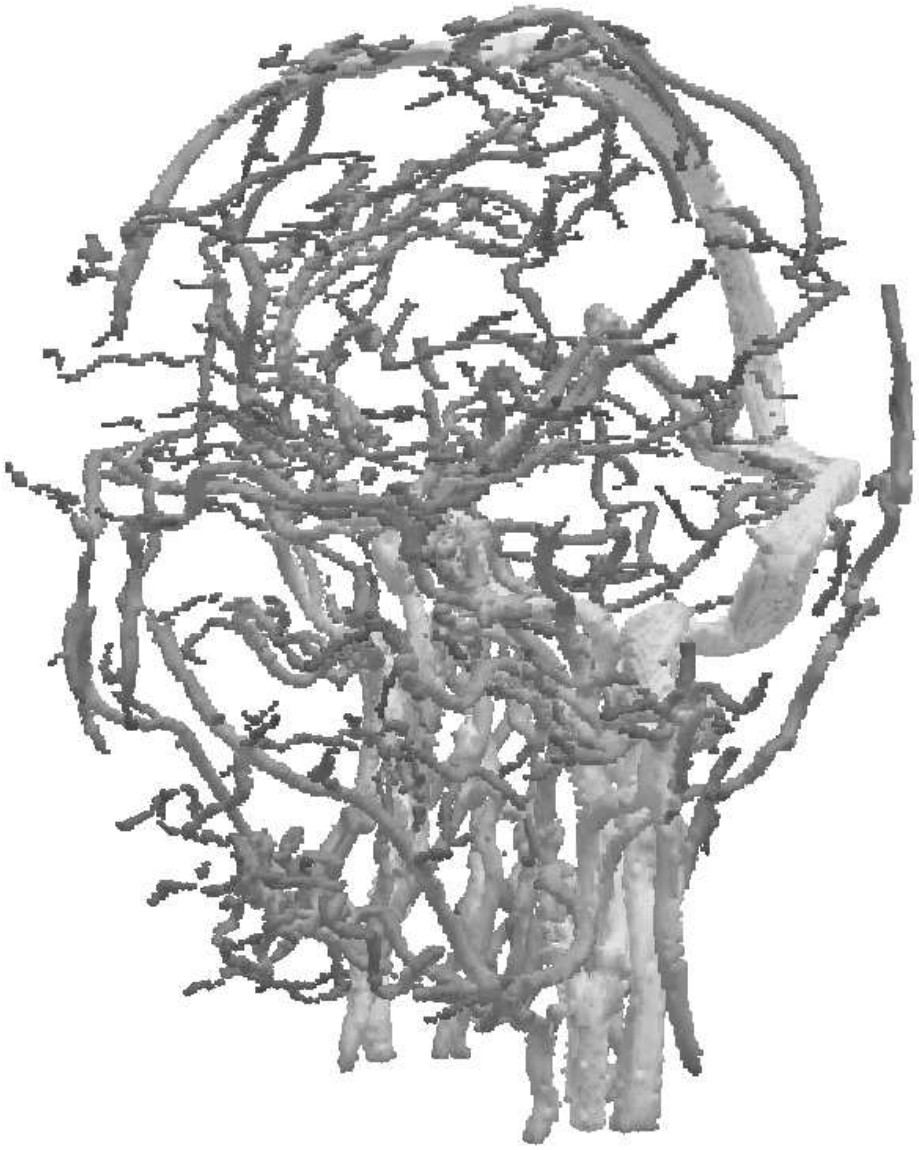

Figure 5. 3D visualization of cerebral vascular trees segmented by the atlas-based algorithm.

7. CONCLUSION

This paper presented a novel method, based on an atlas and an adaptative region growing process, dedicated to blood vessels segmentation in PC-MRA images of the brain and of the whole head. The method has been tested on 15 PC-MRA, providing significantly more precise results than two no atlas-based algorithms. The main originality of this work consisted in using an atlas for vascular segmentation purpose, thus permitting to include a priori anatomic knowledge in order to make the proposed region growing algorithm more adaptative and thus more reliable. Atlas-based segmentation algorithms had already been designed[20] for non vascular brain structures, but never for vascular structures. Indeed, the determination of invariant properties directly on blood vessels is a very hard task, hence forbidding to create an atlas directly on vascular data such as PC-MRA phase images. Thus the proposed atlas, based on a PC-MRA magnitude image, contains information on vessel properties *relatively* to non vascular brain and head structures. This was a first attempt to integrate

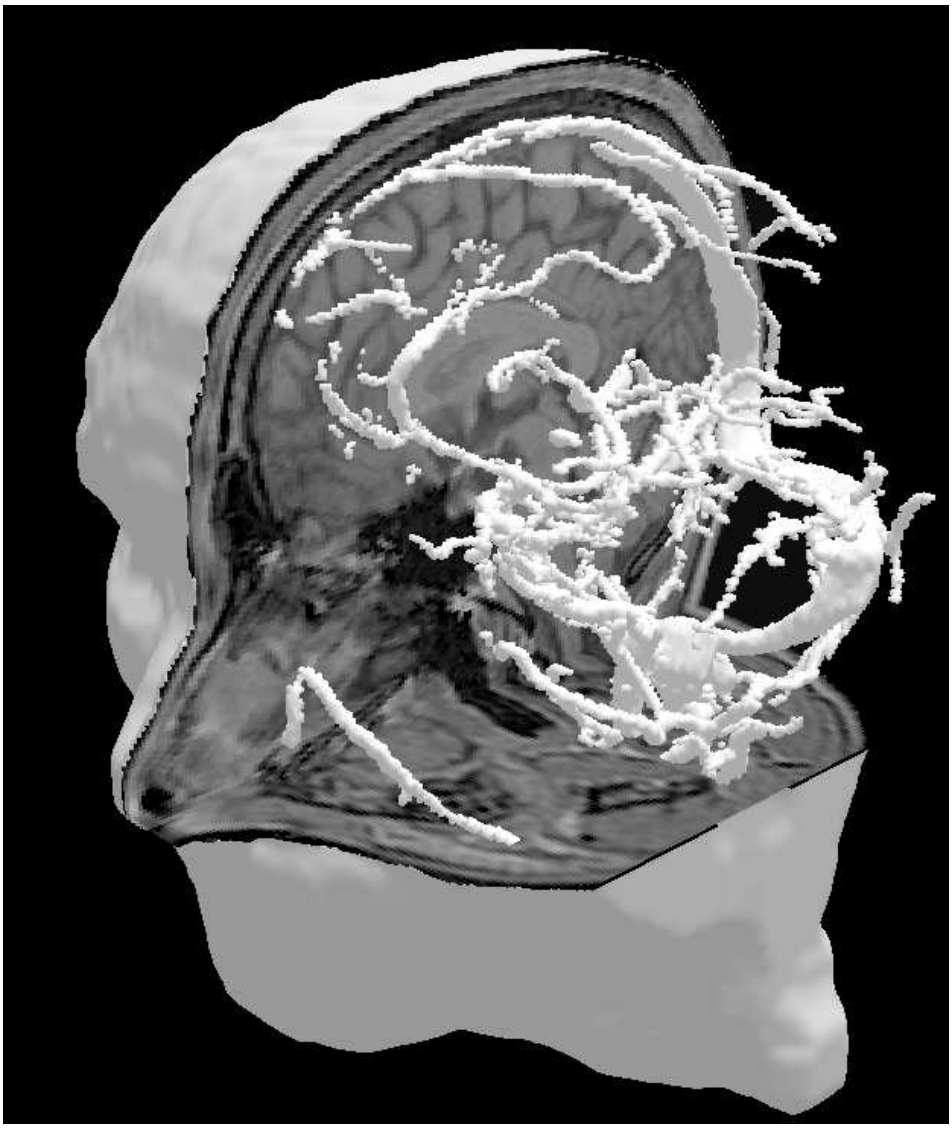

Figure 6. 3D visualization of cerebral vascular trees segmented by the atlas-based algorithm in relation to their environmental anatomical head structures.

anatomical knowledge in a vessel segmentation process. The proposed method and the results it provides, give the proof that anatomic knowledge integration can be a way to increase the efficiency of algorithms dedicated to vascular segmentation. Further studies will consist in optimizing the reliability of the proposed atlas by creating mixed areas at the frontier between different regions, in order to better modelize the probability of a voxel to belong to one region or another. Another kind of threshold value determination will also be developed to make the automatic version of the algorithm more robust. Moreover, the knowledge currently used in the proposed algorithm only concerns the intensity of vascular structures to find. That information is used for dynamic threshold evolution. Other kinds of high-level anatomical knowledge such as vessels orientation and position relatively to non vascular structures, which can be modelized by the atlas will be integrated too. The atlas will then be more intensively used to become the basis of new algorithms dedicated to brain vascular tree segmentation.

8. ACKNOWLEDGEMENTS

The authors thank the EPML IRMC[‡‡] (EPML n°9 CNRS-STIC) for its financial support. They also thank V. Noblet and T. Berst, whose theoretical and technical assistance largely contributed to this work.

REFERENCES

1. C. Dumoulin and H. Hart, "Magnetic resonance angiography," *Radiology* **161**, pp. 717–720, 1986.
2. F. Wehrli, A. Shimakawa, G. Gullberg, and J. McFall, "Time of flight MR flow imaging: selective saturation recovery with gradient refocusing," *Radiology* **160**, pp. 781–785, 1986.
3. C. Dumoulin, S. Souza, M. Walker, and W. Wagle, "Three-dimensional phase contrast angiography," *Magnetic Resonance in Medicine* **9**, pp. 139–149, 1989.
4. M. Orkisz, C. Bresson, I. Magnin, O. Champin, and P. Douek, "Improved vessel visualization in MR angiography by nonlinear anisotropic filtering," *Magnetic Resonance in Medicine* **37**, pp. 914–919, 1997.
5. Y. Du and D. Parker, "Vessel enhancement filtering in three-dimensional angiograms using long-range signal correlation," *Journal of Magnetic Resonance Imaging* **7**, pp. 447–450, 1997.
6. H. Cline, D. Thedens, C. Meyer, D. Nishimura, T. Foo, and S. Ludke, "Combined connectivity and a grey-level morphological filter in magnetic resonance coronary angiography," *Magnetic Resonance in Medicine* **43**, pp. 892–995, 2000.
7. P. Yim, P. Choyke, and R. Summers, "Gray-scale skeletonization of small vessels in magnetic resonance angiography," *IEEE Transactions on Medical Imaging* **19**, pp. 568–576, 2000.
8. S. Kobashi, N. Kamiura, Y. Hata, and F. Miyawaki, "Volume-quantization-based neural network approach to 3D MR angiography image segmentation," *Image and Vision Computing* **19**, pp. 185–193, 2001.
9. C. Zahlten, H. Jürgens, and H.-O.Peitgen, "Reconstruction of branching blood vessels from CT-data," in *Visualization in Scientific Computing*, M. Göbel, H. Müller, and B. Urban, eds., *Springer-Verlag*, pp. 41–52, 1995.
10. P. Dokládal, C. Lohou, L. Perroton, and G. Bertrand, "Liver blood vessels extraction by a 3-D topological approach," in *Proc. MICCAI '99*, 1999.
11. N. Flasque, M. Desvignes, J. Constans, and M. Revenu, "Acquisition, segmentation and tracking of the cerebral vascular tree on 3D magnetic resonance angiography images," *Medical Image Analysis* **5**, pp. 173–183, 2001.
12. Y. Sato, S. Nakajima, N. Shiraga, H. Atsumi, S. Yoshida, T. Koller, G. Gerig, and R. Kikinis, "Three-dimensional multi-scale line filter for segmentation and visualization of curvilinear structures in medical images," *Medical Image Analysis* **2**, pp. 143–168, 1998.
13. K. Krissian, G. Malandain, N. Ayache, R. Vaillant, and Y. Trousset, "Model-based detection of tubular structures in 3D images," *CVIU: Computer Vision and Image Understanding* **80**, pp. 130–171, 2000.
14. L. Lorigo, O. Faugeras, W. Grimson, R. Keriven, R. Kikinis, A. Nabavi, and C.-F. Westin, "CURVES: Curve evolution for vessel segmentation," *Medical Image Analysis* **5**, pp. 195–206, 2001.
15. A. Frangi, W. Niessen, P. Nederkoorn, O. Elgersma, and M. Viergever, "Three-dimensional model-based stenosis quantification of the carotid arteries from contrast-enhanced MR angiography," in *Proceedings of Mathematical Methods in Biomedical Image Analysis 2000*, I. C. S. Press, ed., pp. 110–118, 2000.
16. A. Chung and J. Noble, "Statistical 3D vessel segmentation using a rician distribution," *Lecture Notes in Computer Science* **1679**, pp. 82–89, 1999.
17. D. Wilson and J. Noble, "An adaptive segmentation algorithm for time-of-flight MRA data," *IEEE Transactions on Medical Imaging* **18**, pp. 938–945, 1999.
18. T. Kong and A. Rosenfeld, "Digital topology: introduction and survey," *Computer Vision, Graphics, and Image Processing* **48**, pp. 357–393, 1989.
19. C. Heinrich, V. Noblet, F. Heitz, and J.-P. Armspach, "3-D deformable image registration: a topology preservation scheme based on hierarchical deformation models and interval analysis optimization," *Technical Report, LSIIT, UMR CNRS-ULP 7005* , 2003.
20. O. Musse, F. Heitz, and J.-P. Armspach, "Fast deformable matching of 3D images over multiscale nested subspaces. Application to atlas-based MRI segmentation," *Pattern Recognition* **36**, pp. 1881–1899, 2003.

[‡‡]Équipe-Projet Multi-Laboratoires Imagerie et Robotique Médicale et Chirurgicale; `http://irmc.u-strasbg.fr/`